Effect of thermal conductivities of materials on performance of Swiss-roll combustor

S. Aizumi[1], T. Yokomori[1], Y. Tsuboi[1] S. Kato[2], K. Maruta[1]

[1]Institute of Fluid Science, Tohoku University,
2-1-1 Katahira, Aoba-ku, Sendai, Miyagi 980-8577, Japan

[2]Ishikawajima-Harima Heavy Industries Co., Ltd.
2-2-1 Ohtemachi, Chiyoda-ku, Tokyo 100-8182, Japan

1 Introduction

The higher energy densities of fossil fuels have motivated studies on small combustors to substitute the commercial batteries. However, increasing heat loss due to large surface-to-volume ratio of small combustor provokes flame quenching, which hinders a stabilization of a self-sustained flame. To overcome this difficulty, heat-recirculating combustors were considered to reduce total heat loss[1,2,3]. In heat-recirculating combustors, by transferring thermal energy from combustion products to reactants, the effective incoming enthalpy can be higher than that of cold reactants and stable combustion is possible under the condition where the flame is extinguished without heat recirculation. Our group has developed several sizes of "Swiss-roll" heat-recirculating micro combustors (Fig. 1) as heat sources[4,5]. However, the effects of scales and design parameters on the performance of Swiss-roll combustors were not fully understood and should be clarified from more detailed studies. This study focused on the effect of thermal conductivity of the combustor material on the combustion characteristics.

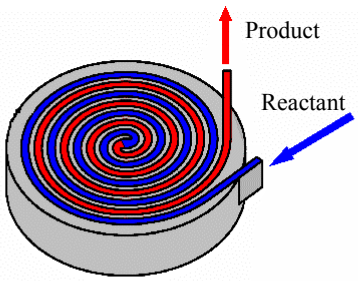

Fig. 1 Schematic of swiss-roll combustor

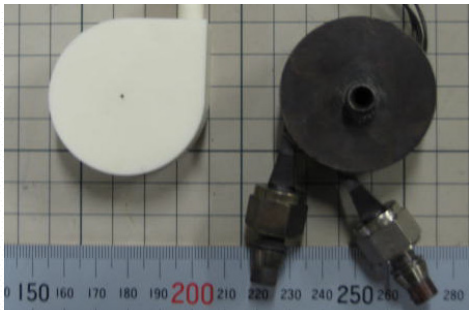

Fig. 2 Photos of small combustors, Left : Small combustor with ceramic, Right : Small combustor with stainless-steel

2 Experimental setup

Based on the previous studies for standard size Swiss-roll combustors (diameter 64mm)[4], scale-down combustors termed "small-combustor" (diameter 46mm) were fabricated with two kinds of materials as shown in Fig. 2 (left: Ceramic, right: Stainless-steel). The channel width, wall thickness and top and bottom plate thicknesses are 1.05 mm, 0.105 mm and 5 mm, respectively. The number of channel turns is 3.5. All surfaces except the upper surface of the combustor were thermally insulated during experiments. A spark igniter was

Correspondence to : maruta@ifs.tohoku.ac.jp

installed at the center of the combustor. Propane/air mixture with equivalence ratio ϕ = 0.9 was used. Temperatures of the upper surface of the combustor were measured with five thermocouples.

3 Experimental results

Figure 3 shows surface temperatures of small combustors as a function of the mean velocity of mixture. These temperatures were obtained after combustors have reached steady states. Steady state is defined here as a state where the variations of all surface temperatures became less than ± 0.2 K/min. The surface temperature of ceramic combustor reaches the maximum (~1050 K) at 450 cm/s. On the other hand, stainless-steel combustor does not show the maximum surface temperature in the permissible temperature range of stainless-steel. Ceramic small-combustor has both upper and lower velocity limits, although stainless-steel combustor does not exhibit upper velocity limit as shown in Fig. 3.

These differences are expected to be due to the different thermal conductivities of materials. Thermal conductivity of stainless-steel increases with the increase of temperature, while that of ceramics decreases with the increase of temperature. In high temperature region (~ 1500K), heat recirculation is not enough for ceramic combustor, because thermal conductivity of ceramic (~ 5 W/m·K) is almost one-seventh to that of stainless-steel (~ 35 W/m·K) [6]. Therefore, maximum surface temperature of the ceramic combustor is lower than that of stainless-steel combustor thus blow-off easily occurs for ceramic combustor.

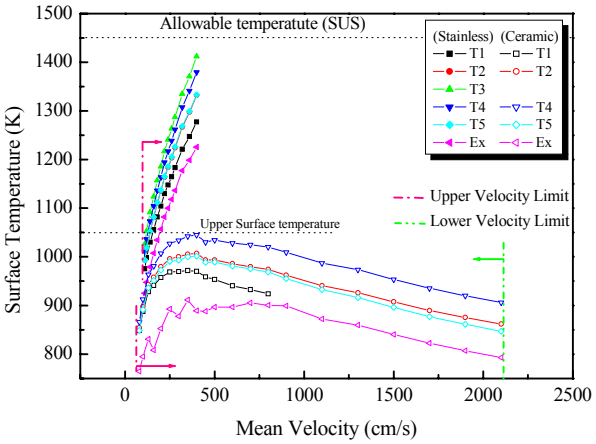

Fig.3 Mean velocity with measured surface temperature

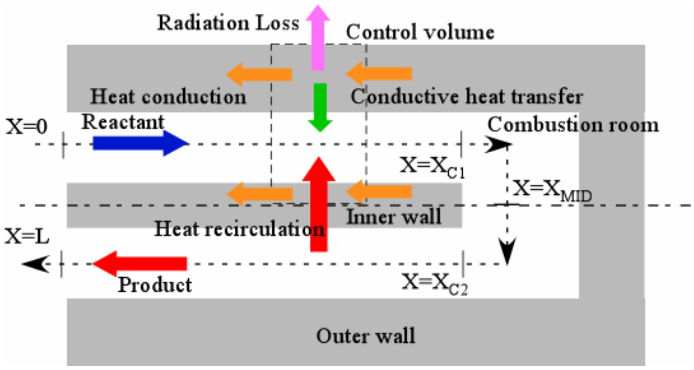

Fig.4 Schematic of computation model

4 Computations

To examine the effects of thermal conductivity on combustion characteristics, a simple model of heat-recirculating combustor (U-shape combustor) shown in Fig. 4 was numerically examined. The combustion room was modeled by the cosine shaped cross sectional area A_g for stabilizing the flame at the center of the combustor.

$$A_g = a - b \times \cos(2\pi / R(X - X_{C1})) \quad (X_{C1} \le X \le X_{C2}), \quad A_g = c \quad (0 \le X \le X_{C1},\ X_{C2} \le X \le L) \quad ...(1),$$

where X_{C1} and X_{C2} were entrance and exit of combustion room. L and R were the length of calculation domain and the length of combustion room, respectively. a , b and c were constants based on the experimental apparatus (a = 0.314 ,b = 0.167 ,c = 0.147). Energy equations for gas and solid phases are shown in Eqs. (2) and (3), respectively.

$$\dot{M}\frac{dT_g}{dx} - \frac{d}{c_p}\frac{d}{dx}\left(k_g A_g \frac{dT_g}{dx}\right) + \frac{A_g}{c_p}\left(\sum_{n=1}^{N}\rho Y_n V_n c_{pn}\frac{dT_g}{dx} + \sum_{n=1}^{N}\dot{\omega}_n\right) - \frac{A_c}{c_p}h\left(T_S - T_g\right) = 0 \quad ...(2),$$

$$\frac{d}{dx}\left(k_s A_s \frac{dT_s}{dx}\right) - A_c h\left(T_s - T_g\right) - A_r \sigma \varepsilon \left(T_s^4 - T_a^4\right) + Q_{re} = 0 \ldots(3),$$

$$Q_{re} = A_{re} k_s \frac{T_s(X_{MID} + \Delta x) - T_s(X_{MID} - \Delta x)}{t_w} \ldots(4),$$

where subscript g and s denote gas and solid. k, T and $\dot{M}$ are thermal conductivity, temperature and the mass flow rate through the channel, respectively. The convective heat transfer coefficient was defined as $h = Nuk_g / W_h$ and the Nusselt number was assumed as 4. Hydraulic diameter was defined as $W_h = 2A_c/(w+d)$. w and d represent channel width and depth. A_g and A_s are cross sectional areas for gas and solid phases. A_c, A_r and A_{re} represent convective heat transfer, radiation loss and heat recirculation area of the control volume, respectively. Heat loss from the combustor surface was considered as radiative heat transfer to the ambient at 300 K.

Heat recirculation perpendicular to the flow direction in the inner wall was considered by Eq. (4). X_{MID} is the center location of the calculation domain, Δx represents the distance from X_{MID} to the control volume and t_w is the thickness of the inner wall. The length of calculation domain was 53.7 cm.

Steady one-dimensional flames with the above heat recirculation were solved by using CHEMKIN-based code with C1-chemistry[7], and methane/air mixture with $\varphi = 1.0$ was used. Fuel is different between experiment and numerical simulation. Propane was used in the experiments for higher stability of proto-type combustor based on its higher heat value per unit volume. Methane is employed for current computations, however, by taking the advantage of reasonable computational load. This difference does not break any generalities of the present computational results.

5 Computation results

Figures 5 (a) and (b) show temperature distributions of gas and solid phases with k_s =5 W/m·K and k_s = 100 W/m·K when the mean velocities are 350 cm/s. The wall temperature distribution in x direction for k_s = 100 W/m·K becomes flatter than that for k_s = 5 W/m·K, and also the wall peak temperature for k_s=5W/ m·K becomes lower. Furthermore, the wall temperature difference between the reactant and the product sides becomes smaller

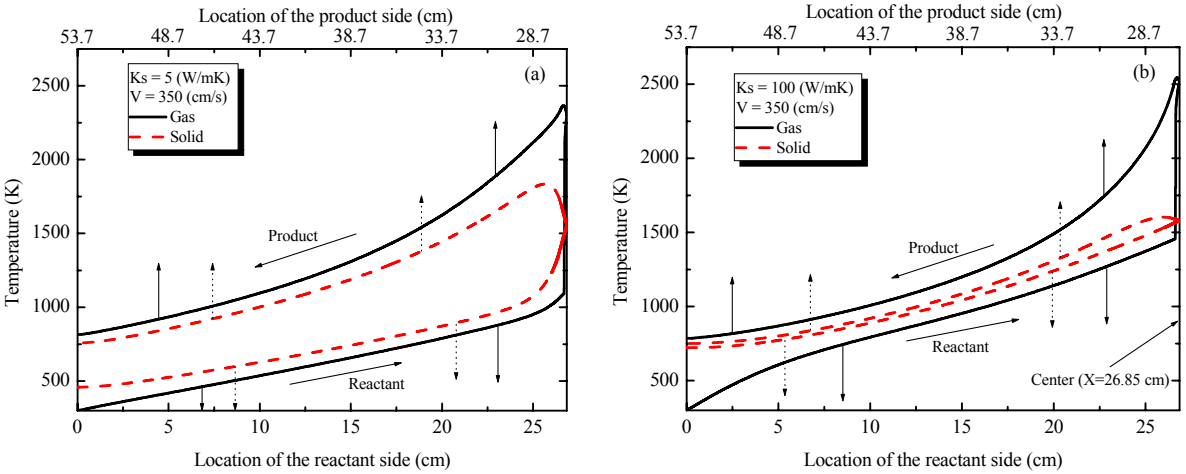

Fig.5 Temperature profile of gas and solid phase at V=350 (cm/s), left (a) : Ks=5 (W/mK) right (b) : Ks=100 (W/mK)

for k_s =5 W/m·K.

Figure 6 shows the flame temperature defined as the gas peak temperature as a function of the mean velocity for various thermal conductivities. The flame temperatures exhibit the maximum for all thermal conductivities, for example, it is 2400 K at 220 cm/s for k = 5 W/m·K. The velocity at the maximum flame temperature increases with the increase of thermal conductivity. Furthermore, the maximum flame temperature increases with

the increase of thermal conductivity when $K_s \leq 100$ W/m·K, while the maximum flame temperature decreases significantly when K_s=400 W/m·K.

Figure 7(a) shows the effect of thermal conductivity of the combustor on blow off limits. The figure shows that 1) when $K_s \leq 100$ W/m·K, blow off limit increases with the increase of thermal conductivity, and 2) when $K_s > 100$ W/m·K, blow off limit decreases gradually. This is due to the difference of flame temperature. Since the combustor with low thermal conductivity has low flame temperature, blow off occured easily at low velocity as observed in the ceramic combustor experiment.

Figure 7(b) shows the effect of thermal conductivity of the combustor on flash back and low velocity quenching limits. When $K_s \leq 100$ W/m·K, flame could propagate into upstream channel out of combustion room. On the other hand, quenching occur within the combustion room when $K_s > 100$ W/m·K and flame never propagated into upstream channel. This is because the solid temperature at the combustion room (X=26.5 – 27.2cm) with high thermal conductivity is lower than that with low thermal conductivity. Therefore, heat loss from the flame to the solid wall is larger and it is difficult for the flame to propagate and self-sustain.

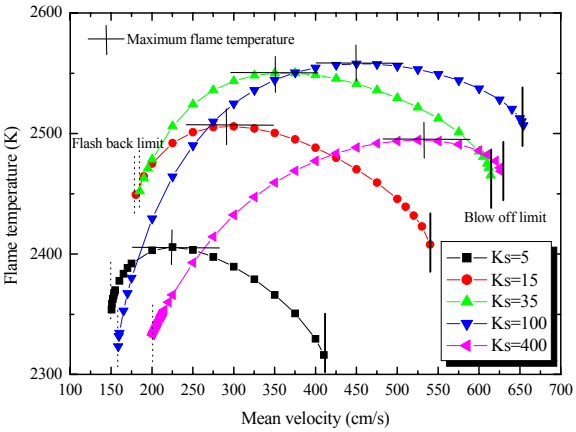

Fig.6 The effect of the thermal conductivities of solid on flame temperature

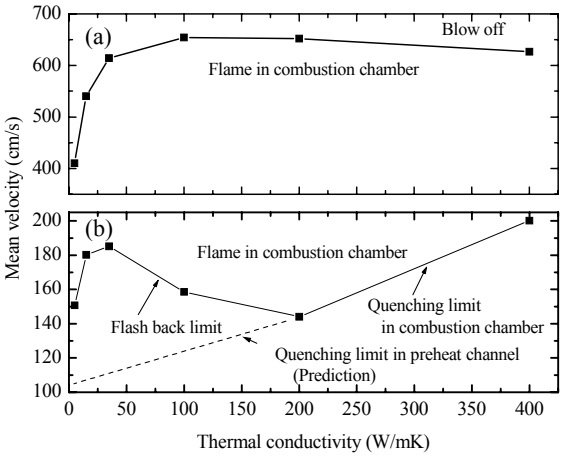

Fig.7 (a) Blow off limit with thermal conductivity of combustor. (b) Flash back and quenching limit with thermal conductivity of combustor

6 Conclusions

1. The present experiments showed that combustion characteristics strongly depend on thermal conductivity of combustor materials.
2. The effect of thermal conductivity on flame temperature and stability limits were confirmed by computations. Computations suggested that the existance of optimum thermal conductivity for the effective heat recirculation.
3. When $K_s \leq 100$ W/m·K, blow off limit increases with the increase of thermal conductivity, and the flame could propagate to upstream channel out of combustion room in low velocity.
4. When $K_s > 100$ W/m·K, blow off limit decreases gradually and the quenching occur within the combustion room in low velocity.

References

[1] S. A. Lloyd, F. J. Weinberg, Nature, 251, 47(1974)
[2] J. Ahan, C. Eastwood, L. Sitzki, P. D. Ronney, Proc. Combut. Inst. 30 (2005) 2463-2472.
[3] M. Chen and J. Buckmaster, Combust. Theory Modelling 8 (2004) 701-720.
[4] N. I. Kim, T. Yokomori, T. Fujimori, K. Maruta, et al., Combust. Flame 141 (2005) 229-240.
[5] N. I. Kim, T. Yokomori, T. Fujimori, K. Maruta, et al., Development and scale effects of small Swiss-roll combustors, Proc. Combust. Inst. (2007), doi :10.1016/j.proci.2006.08.043
[6] Frank P. Incropera and David P. Dewitt. Fundamentals of Heat and Mass Transfer, 5th edit.
[7] R. J. Kee, et al, Sandia Report, SAND85-8240.